Journal of Power Sources 198 (2012) 378–382

Contents lists available at SciVerse ScienceDirect

Journal of Power Sources

journal homepage: www.elsevier.com/locate/jpowsour

Short communication

New high-energy lead-acid battery with reticulated vitreous carbon as a carrier and current collector☆

Andrzej Czerwiński[a,b,*], Szymon Obrębowski[a,b], Zbigniew Rogulski[a,b]

[a] Industrial Chemistry Research Institute, Rydygiera 8, 01-793 Warsaw, Poland
[b] Department of Chemistry, University of Warsaw, Pasteura 1, 02-093 Warsaw, Poland

ARTICLE INFO

Article history:
Received 19 August 2011
Received in revised form
12 September 2011
Accepted 23 September 2011
Available online 1 October 2011

Keywords:
Lead-acid battery
RVC
Porous carbon material
Grid

ABSTRACT

2 V lead-acid cell employing RVC galvanized with Pb as the grid material has been designed and tested. Two thick (>0.5 cm) plates have been used for assembling prototype flooded cell. It completed over 65 charge/discharge cycles at 50% depth of discharge without losing its nominal capacity. For higher discharge currents at 100% DOD the cyclic lifetime is limited as a result of grid corrosion which is probably due to relatively thin, non-alloyed pure lead grid coating. However, very promising capacity values for 20-h discharge rate at the level of 120 A h kg^{-1} PAM, 170 A h kg^{-1} NAM have been obtained, the high current response is still below the expectations. Average internal resistance of the new cells is 45 mΩ, which is in parallel with limited high-current response. Perspective of designing serial lead acid cell employing lightweight reticulated carbon as a grid material is clearly visible. There is a need of introducing high-quality, corrosion resistant Pb-alloy for RVC coating and lowering the plates thickness for better high current performance.

1. Introduction

Due to simple and non-expensive technology lead-acid batteries (LABs) are still most common electrochemical power sources in many medium and large-scale energy-storage applications [1]. The main disadvantage of lead-acid battery system in comparison to other battery systems is low specific capacity (A h kg^{-1}). Except of high density of Pb and PbO_2 electroactive material, the main reason of this property is the high contribution of plate grid to the total plate mass. Depending on the type of the lead-acid battery, the battery specific capacity and specific energy average values are 14–17 A h kg^{-1} and 30–35 W h kg^{-1}, respectively [1,2]. Specific energy performance at the level of 50 W h kg^{-1} (level of Ni–Cd batteries) would open the possibility of introducing lead batteries for road EV/HEV. The possible approach to overcome the problem of relatively low specific capacity and energy of lead acid batteries is employing lightweight porous carbon materials coated with metals especially lead/lead alloys as current collectors. This idea was first proposed by Czerwiński and co-workers [3–9] who has used the reticulated vitreous carbon (RVC) as current collector and carrier for active mass as an alternative for lead alloy cast grids. Reticulated vitreous carbon (RVC) is brittle and has lower conductivity than graphite, however, it is chemically inert and has much higher void volume than porous graphite with corresponding porosity [10]. RVC was applied in many primary and secondary battery systems [11,12]. Since mid-nineties different types of porous carbon materials have been investigated as base material for lead acid battery plates [3–9,13–21]. The plate design based on reticulated vitreous carbon was adapted further by Gyenge et al. [13,14] who constructed a lead-acid battery using RVC covered with lead alloys. Other carbon materials have been also proposed as an active mass carrier and current-collectors mainly for negative plates in lead-acid batteries. Chen and co-workers have used carbon foam [15–18] in a lead-acid battery system. Recently, it has been demonstrated that RVC covered and non-covered with lead has excellent behavior as a carrier and current collector in negative plate of lead-acid battery [20]. The Pb/RVC negative plate has been mounted in complete 2 V lead-acid battery containing one negative RVC-based plate and two positive plates from commercial battery. The electrical capacity, charging–discharging behavior, Peukert's plots and other parameters have proved that this hybrid lead-acid battery can compete with batteries with lead alloy carriers [20,21]. Carbon matrix has to be mechanically and chemically separated from active PbO_2 mass due to oxidation reactions during positive plate charging and high oxidation standard potential of PbO_2. It has been

☆ This publication is based on the results presented at the LABAT 2011 Conference.

* Corresponding author at: Department of Chemistry, University of Warsaw, Pasteura 1, 02-093 Warsaw, Mazowsze, Poland. Tel.: +48 022 8222011; fax: +48 022 8225996.
E-mail address: aczerw@chem.uw.edu.pl (A. Czerwiński).

0378-7753/$ – see front matter © 2011 Elsevier B.V. All rights reserved.
doi:10.1016/j.jpowsour.2011.09.081

demonstrated that RVC with surface fully covered with lead can be used as carrier and current collector also in positive plates of lead-acid battery [22,23].

The aim of our work was to design, assemble and test complete 2 V cells with significantly lowered mass by employing lead electroplated RVC matrix as a carrier and current collector for both positive and negative plates. In this paper a new construction of lead-acid battery and its preliminary performance is demonstrated.

2. Experimental

The negative and positive plates were prepared from 20 p.p.i. (pores per inch) RVC block which was cut into small substrates with average dimensions 2.5 cm × 4 cm × 0.5 cm. Electrical contact was made from thin Pb wires (d = 0.5 mm) [25,26]. Average weight of the RVC substrate with electrical contact varied between 1.4 g and 1.6 g. Before pasting the RVC carrier has been electrochemically covered with lead from alkanesulphonate bath. Lead layer thickness covering the RVC matrix was 60 μm (positive collector) and 20 μm (negative collector). Plates were prepared by manual pasting the negative and positive masses into the Pb/RVC current collector. Fresh negative and positive pastes were obtained from JENOX Ltd. lead-acid battery manufacturer. Before applying to grids, pastes were slightly diluted with water in order to enable pasting of thick reticulated grid. After pasting, the electrodes thickness was 5–6 mm. Plates were then subjected to two-step curing process lasting 24 h in 45 °C at 90% relative humidity and drying in 45 °C for the next 24 h. The amount of positive active mass after curing process was 18.0 ± 0.5 g, the amount of negative active mass was 12.4 ± 0.2 g. BET surface of PAM measured after curing is 1.50 $m^2\ g^{-1}$. Morphologies of the RVC® and Pb surfaces were examined with a LEO 435VP scanning electron microscope (SEM). The cured plates were separated with the SLI-type polyethylene ribbed separator and compressed in the polypropylene casing. Then the casing was heat-sealed tightly with the PP cover through which electrical terminals were conducted. In purpose of cell watering or electrolyte exchanging a little space was left between the terminals and polypropylene cover. After soaking for 4 h in H_2SO_4 electrolyte (d = 1.15 g cm^{-3}) at a temperature of 40 °C the formation process was performed in 1.15 g cm^{-3} H_2SO_4 using constant current method until 6.24 A h charge passed through the cell. Based on our previous findings, the nominal capacity of prototype cells was predicted on 2 A h. After formation, acid density was adjusted to 1.26 g cm^{-3} H_2SO_4. Discharge tests at different current rates were performed in H_2SO_4 electrolyte with d = 1.26 g cm^{-3} using Atlas-Sollich 0961 battery tester. The total mass of the complete cell was 85 ± 2 g. Constant current–constant voltage charging was performed with 160 mA current followed by 2.4 V constant voltage step until the current drop below 100 mA (0.05C). For life cycle tests at 50% DOD constant voltage charge step at 2.4 V was prolonged to 7 h. Internal resistance was measured using the impedance spectrometry. Voltage amplitude applied to cell was 50 mV against the OCV (2.12 V) and frequency range was 100 kHz to 0.1 Hz.

3. Results and discussion

Fig. 1 presents lead surface electrodeposited on RVC from methanesulphonate bath. It is possible to see that big, flat lead crystals are surrounded with narrow cracks. Although the structure of the layer is not as uniform as cast leads', the crystals seem to be packed tight enough to resist the potential cycling in corrosive acidic environment.

Fig. 2 presents complete, cured negative and positive plate employed in our cell. The scheme of a complete two-plate 2 V cell is presented in Fig. 3. In Table 1 the weight mass analysis of the main

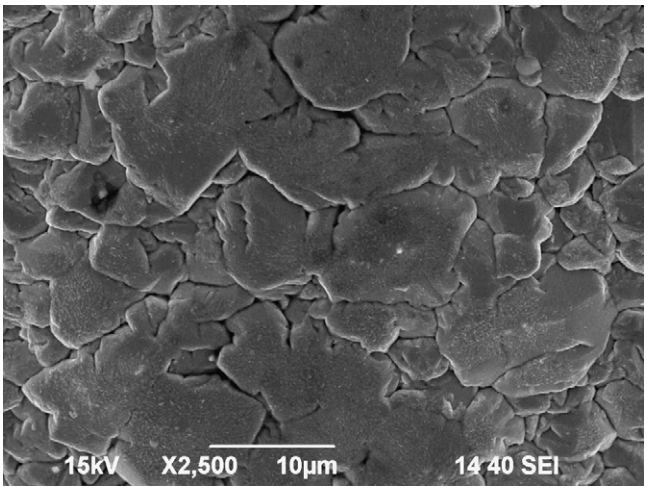

Fig. 1. Surface of Pb galvanic layer deposited on RVC from methanesulphonate bath.

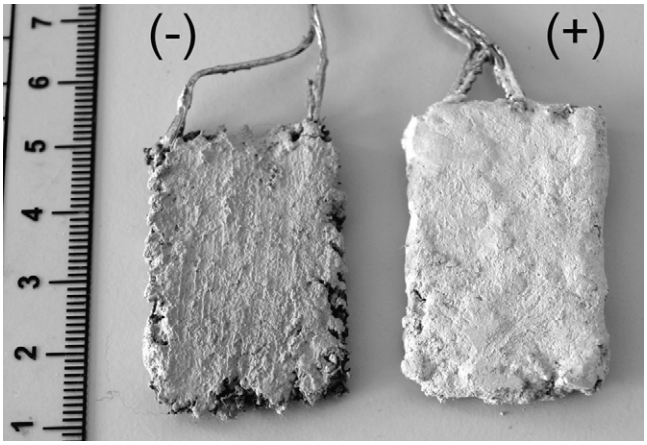

Fig. 2. Positive and negative plate employed in prototype 2 V, 2 A h cell.

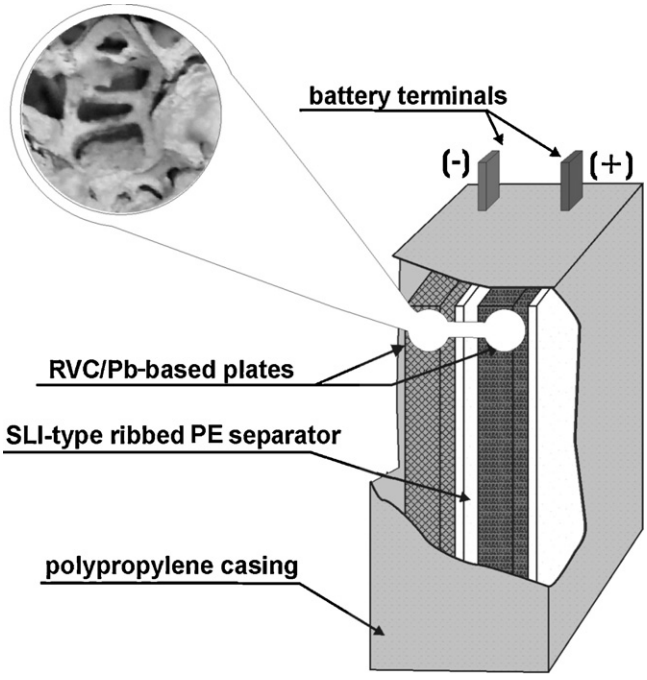

Fig. 3. Scheme of our prototype 2 V, 2 A h cell. Cured RVC/Pb-based plate magnified in the circle.

Table 1
Weight analysis of prototype cells components.

Negative collector	Negative active mass	Positive collector	Positive active mass	Separator	Electrolyte	Container	Top lead
3 g (4%)	13 g (16%)	4 g (5%)	18 g (20%)	1 g (1%)	27 g (31%)	10 g (12%)	9 g (11%)

constructing elements in new lead-acid battery is presented. The component participation in total mass of the constructed battery is enclosed in brackets.

The values in Table 1 show very low contribution of masses of collectors to the total battery mass which is less then 10% in comparison to ca. 25–30% in batteries with standard cast grids.

The cell was flooded with an excess of electrolyte, therefore the acid weight contribution is relatively high. Container and top lead masses have not been optimized but the masses seem to have reasonable values. Very important plate construction parameters which have to be controlled in the process of plate development are gamma coefficient (γ) [24] and grid-to-plate ratio N (%). As it is shown in Table 1, the negative plates are pasted with little less amount of mass than positives. Gamma coefficient equals 0.35 g cm^{-2} for negative and 0.5 g cm^{-2} for positive plate, respectively. This difference gives an advantage of better NAM efficiency. The N factor is 5% for negative plate and 16% for positive which is much lower than for standard plates based on cast grids (N = 40%). Formation current 0.16 A has been estimated empirically. For this current the positive plate turns brown evenly in the whole volume at the end of formation process. After cracking it half there are few small dots (ca. 0.2 mm diameter) of white Pb^{2+} species spread irregularly in the active mass. The surface colour is brown. The higher the formation current the more white crystals of Pb^{2+} species are present in the plate. For currents as high as 400 mA after 2 days of formation the plate surface is chocolate brown but the interior shows visible gradient of colour. White sulphate builds the plate core. The plate colour becomes more brown towards the surface.

In order to determine nominal capacity of the cell after its formation the cell was subjected to three charge/discharge cycles at discharge current 100 mA (20 h of discharging mode, 0.05C) while charging was performed for 17 h with 160 mA current. The capacity of eight prototype cells varies between 93% and 106% of nominal 2 A h which gives average value of 2.03 A h. This value shows that plates have been formed completely and the nominal capacity has been predicted on the good level. Average specific capacity per total cell mass equals 24.4 A h kg^{-1}.

Internal resistance of prototype cells has been measured by using the impedance spectrometry technique. R values were taken after the first and sixth charge for two tested cells. The change between cell's internal resistance is negligible and was averaged. Fig. 4 shows the impedance spectra of charged cell after the first and sixth 0.05C cycle.

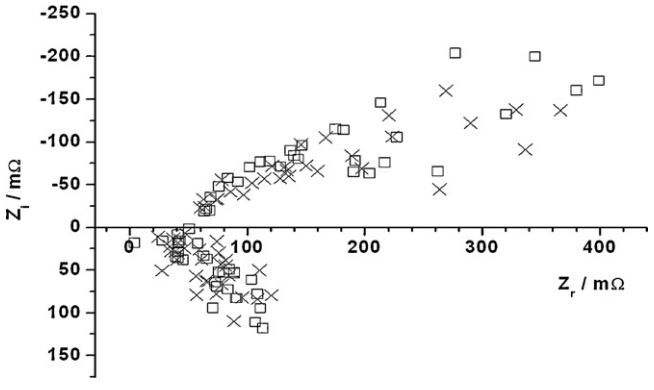

Fig. 4. Impedance spectra of prototype lead-acid cell after formation (crosses) and after the sixth charge/discharge cycle (squares) at 100% DOD.

Values of the real resistance are on the level acceptable for lead acid cells, however, slightly higher than expected for 2 V, 2 A h single cell. The internal resistance values for 8 cells vary between 30 and 60 mΩ with the average value of 45 mΩ. It is reasonable to claim that the main contribution to the internal resistance has the lead galvanic layer. Introducing alloying elements like tin and silver will definitely lower the grid resistance causing better overall performance of our prototype cell. One also has to remember that we used production routines suited for thin automotive plates. Optimization of paste composition and curing procedure to suit our thick, RVC-based plates will also lower cells' internal resistance.

Fig. 5 presents discharge profiles of prototype batteries. However, voltage level during discharge at 0.05C rate is relatively good comparing to lead-acid battery standards, discharge voltage and discharge capacity for elevated currents is shorter than it should be for 2 A h cell. There are several possible reasons for observed behavior. First, the cell is assembled with plates which are relatively thick comparing to their 2 A h capacity. For high current rate the acid is consumed much faster than is being fed to the plate interior. As a result the gradient of acid concentration in the direction towards interior of the plate is likely to occur. Acid diffusion is also hindered by the lead sulphate layer itself precipitating at the plate surface. PAM surface in contact with concentrated electrolyte is limited. As a result discharge voltage is lower and overall plate capacity is lower than for thin plates.

It is possible to influence high current behavior by optimizing plate construction (introducing several points of top lead connection with the plate collector), geometry (i.e. reducing plate thickness). It is also known that introducing several step formation with high current step for 3BS pastes would influence positively PAM surface which results in lower internal resistance and higher high current capacity. Fig. 6 shows Peukert's dependence normalized to average total cell mass (85 g). The capacity values for 0.05C are very good, better than for commercial VRLA batteries.

Positive and negative plate charge efficiencies are presented in Fig. 7. Due to great NAM to grid surface ratio (0.35 g cm^{-2}) negative plate discharge capacity is very high. This good result is also due to 3D structure of RVC which improves the electric conductivity in the bulk of the active mass. The positive plate discharge capacity is at the expected 120 A h kg^{-1} for 20-h discharge. It is known that lowering the amount of active masses results in their better utilization and thus gives a possibility of better cell design.

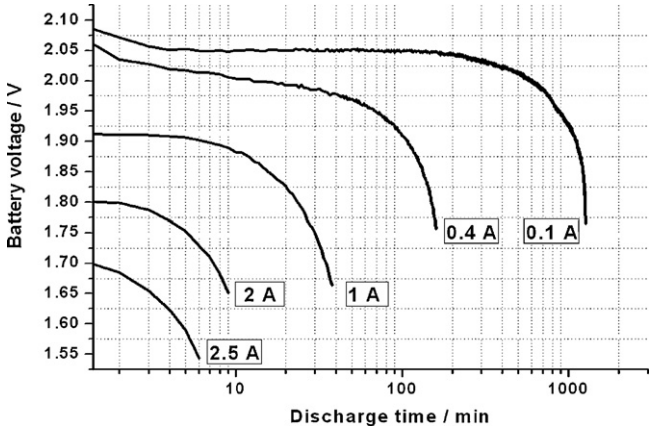

Fig. 5. Battery voltage plotted versus discharge time at different current rates.

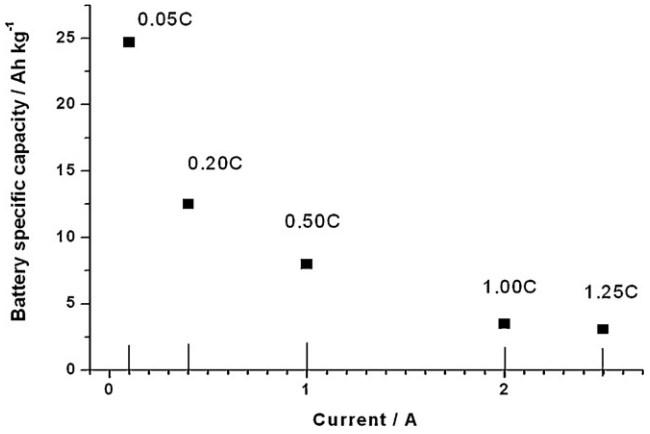

Fig. 6. Discharge capacity of 2 A h, 2 V prototype battery plotted versus discharge current.

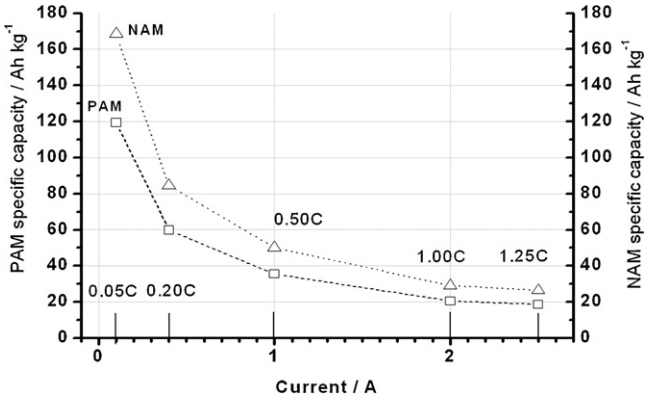

Fig. 7. Active masses discharge capacity plotted versus discharge current: triangles, negative active mass (NAM); squares, positive active mass (PAM).

Cyclic performance of the cell was tested with 100 mA discharge current for 10 h. Those conditions relate to 50% depth-of-discharge. After every 20th cycle 0.05*C* capacity was measured. Charging was performed using constant current 160 mA to reach 2.4 V and cell polarization at 2.4 V for 7 h. The purpose of long time charging at constant potential was to simulate mild overcharging that occurs often during the standard battery duty. Prolonged charge at relatively high constant potential 2.4 V reduces battery cycle life by promoting positive plate collector corrosion. 20-h battery capacity is plotted against cycle number in Fig. 8.

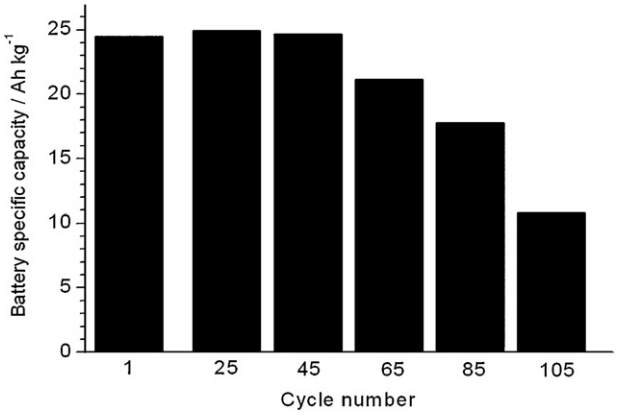

Fig. 8. Battery specific capacity at 0.05*C* constant current discharge rate plotted versus cycle number (DOD 50%).

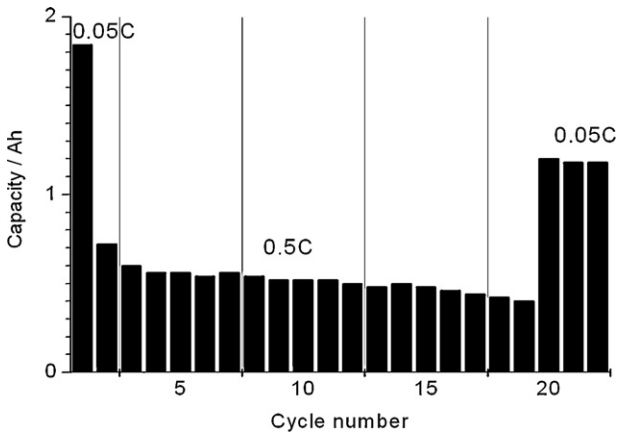

Fig. 9. Battery specific capacity at 0.05*C* and 0.5*C* constant current discharge rate plotted versus cycle number (DOD 100%).

It can be observed that the cell life is at the level of 65 cycles. After completing 105 cycles the cell was disassembled to estimate its condition and the reason of failure. The positive plate was visibly deteriorated. Lead contact wire was corroded and lost the electrical contact with the collector. Active mass was very soft and shedding off the plate heavily. The negative plate survived the cycling without losing mechanical parameters. It should be noticed that active mass has great tendency to shed because low density 3BS paste was used. It is also widely known that pure Pb grids show limited performance in cyclic applications because of specific corrosion processes that occur in the corrosion layer. The parallel reason of limited cycle life is also relatively thin Pb coating on positive plate RVC matrix, which is 60 μm. Using lead alloy coatings with slightly greater thickness are expected to give cyclic life at significantly higher level of charging–discharging cycles, appreciable for small and medium LABs. The experiments are in progress and will be the subject of the next paper.

In order to estimate cell cyclic lifetime in heavy duty conditions we applied 0.5*C* (1 A) constant current discharge. Two step charging method was applied with 160 mA current followed by 2.4 V charge until the current drop below 0.05*C*. Plot presented in Fig. 9 shows typical performance of our battery at 100% DOD.

One can see that after 20 cycles the capacity drops to about 65% of the initial value. After completing this number of cycles the cell was disassembled. The positive plate keeps its rigidity. However, the active mass is softer than right after the formation and it does not contaminate the electrolyte. It is well known that batteries with pure lead grid hardly recover from deep discharge. Out of several possible reasons for that, the most probable is the cracking of corrosion layer due to stresses that result from the cyclic oxidation and reduction of pure lead. The active mass tends to lose its adhesion to the grid which results in relatively fast capacity drop. As mentioned before, this negative behavior can be diminished by pure lead layer replacement on lead alloy.

4. Conclusions

The results obtained for 2 V lead-acid battery based on RVC matrix are preliminary. Changes in galvanic layer phase composition, plating quality and plate construction are expected to improve the prototype battery performance. The demonstrated results can be summarized as follows:

1. A complete 2 V cell with electrical capacity 2 A h has been designed and tested. Obtained 24–25 A h kg^{-1} at 20-h capacity is much better in comparison to lead acid batteries with lead alloy carriers.

2. Elevated negative plate efficiencies (170 A h kg^{-1}) have been obtained due to employment of reticulated grid. It is due to 3D structure of RVC which improves the charge acceptance of the active mass.
3. Internal resistance of the cells is approximately twice as high as of commercial 2 V, 2 A h lead acid cells. This results in limited performance at high current rate.
4. Cyclic lifetime at 0.05*C*, 50% DOD with continuous overcharging is at the level of 65 cycles. Therefore, demonstrated grid has not yet been optimized for cyclic work.
5. For higher discharge currents at 100% DOD the cyclic lifetime is limited due to high thickness of plates which limits the electrolyte penetration in the pores of the bulk of active mass.
6. Prolonged charge at relatively high constant potential 2.4 V reduce battery cycle life by promoting positive plate collector corrosion especially for pure lead grids which have to be replaced on lead alloy.

Acknowledgements

The authors would gratefully acknowledge support from Warsaw University, Industrial Chemistry Research Institute in Warsaw and the Ministry of Science and Higher Education (grant no. N204 135838). The authors also gratefully acknowledge the help of the JENOX Akumulatory Ltd. (Chodzież, Poland)—a leading Polish battery producer in preparation of the complete plates. Current project was realised with the Centre for Preclinical Research and Technology Infrastructure.

References

[1] D. Linden, T.B. Reddy, Handbook of Batteries, McGraw-Hill, New York, 1993.
[2] D.A.J. Rand, P.T. Moseley, J. Garche, C.D. Parker, Valve-Regulated Lead-Acid Batteries, Elsevier, Amsterdam, 2004.
[3] A. Czerwiński, Patent RP, No. 167796.
[4] A. Czerwiński, M. Żelazowska, Patent RP, No. 178258.
[5] A. Czerwinski, M. Żelazowska, Patent RP, No. 180939.
[6] M. Żelazowska, A. Czerwinski, Extended Abstracts, LABAT, 1996, pp. 107–110.
[7] M. Żelazowska-Zakrent, A. Czerwiński, J. Electroanal. Chem. 410 (1996) 53–60.
[8] M. Żelazowska-Zakrent, A. Czerwiński, J. Power Sources 64 (1997) 29–34.
[9] I. Paleska, R. Pruszkowska-Drachal, J. Kotowski, Z. Rogulski, J.D. Milewski, A. Czerwinski, J. Power Sources 129 (2004) 326–329.
[10] ERG Materials and Aerospace Corporation, Duocel® Foam Properties, http://www.ergaerospace.com/foamproperties/introduction.htm.
[11] A. Czerwiński, Z. Rogulski, H. Siwek, S. Obrębowski, I. Paleska, M. Chotkowski, M. Łukaszewski, J. Appl. Electrochem. 39 (2009) 559–567.
[12] Z. Rogulski, W. Lewdorowicz, W. Tokarz, A. Czerwiński, Pol. J. Chem. 78 (2004) 1357–1370.
[13] E. Gyenge, J. Jung, B. Mahato, J. Power Sources 113 (2003) 388–393.
[14] E. Gyenge, J. Jung, Patent No. WO 03028130.
[15] Y. Chen, B.Z. Chen, L.W. Ma, Y. Yuan, Electrochem. Commun. 10 (2008) 1064–1066.
[16] Y. Chen, B.Z. Chen, L.W. Ma, Y. Yuan, J. Appl. Electrochem. 38 (2008) 1409–1413.
[17] Y. Chen, B.Z. Chen, X.C. Shi, H. Xu, W. Shang, Y. Yuan, L.P. Xiao, Electrochim. Acta 53 (2008) 2245–2249.
[18] L.W. Ma, B.Z. Chen, Y. Chen, Y. Yuan, J. Appl. Electrochem. 39 (2009) 1609–1615.
[19] Y. Jang, N.J. Dudney, T.N. Tiegs, J.W. Klett, J. Power Sources 161 (2006) 139.
[20] A. Czerwiński, S. Obrębowski, J. Kotowski, Z. Rogulski, J.M. Skowroński, P. Krawczyk, T. Romanowski, M. Bajsert, M. Przystałowski, M. Buczkowska-Biniecka, E. Jankowska, M. Baraniak, J. Power Sources 195 (2010) 7524–7530.
[21] A. Czerwiński, S. Obrębowski, J. Kotowski, Z. Rogulski, J.M. Skowroński, P. Krawczyk, T. Romanowski, M. Bajsert, M. Przystałowski, M. Buczkowska-Biniecka, E. Jankowska, M. Baraniak, J. Rotnicki, M. Kopczyk, J. Power Sources 195 (2010) 7530–7534.
[22] A. Czerwiński, S. Obrębowski, Z. Rogulski, J. Kotowski, LABAT 2011 Extended Abstracts, 2011, pp. 37–41.
[23] A. Czerwiński, S. Obrębowski, Z. Rogulski, J. Kotowski, LABAT 2011 Extended Abstracts, 2011, pp. 41–45.
[24] D. Pavlov, J. Power Sources 53 (1995) 9–21.
[25] A. Czerwiński, S. Obrębowski, J. Kotowski, M. Bajsert, M. Przystałowski, Z. Rogulski, Patent pending P-387975 (2009).
[26] A. Czerwiński, S. Obrębowski, J. Kotowski, M. Bajsert, M. Przystałowski, Z. Rogulski, Patent pending P-387976 (2009).